APPLIED PHYSICS LETTERS **93**, 071908 (2008)

Blue and red electroluminescence of Europium-implanted metal-oxide-semiconductor structures as a probe for the dynamics of microstructure

L. Rebohle,[a] J. Lehmann, S. Prucnal, A. Kanjilal, A. Nazarov,[b] I. Tyagulskii,[b] W. Skorupa, and M. Helm
Institute of Ion Beam Physics and Materials Research, Forschungszentrum Dresden Rossendorf, POB 510119, D-01314, Germany

(Received 4 June 2008; accepted 2 July 2008; published online 22 August 2008)

The strong blue and red electroluminescence from Eu-implanted SiO_2 layers were investigated as a function of implantation and annealing conditions. It is shown that the red electroluminescence assigned to Eu^{3+} ions is favored by low Eu concentrations, low annealing temperatures, and short annealing times. Based on a more quantitative analysis of the electroluminescence spectra this preference is explained by a shorter supply of oxygen for higher Eu concentrations and the growth of Europium or Europium oxide clusters with increasing annealing temperatures and annealing times. The correlation between electroluminescence and microstructure is supported by transmission electron microscopy investigations and demonstrates that the electroluminescence of Eu-implanted SiO_2 layers can serve as a probe for the microstructural development in the active layer of the light emitter. © *2008 American Institute of Physics*. [DOI: 10.1063/1.2964176]

Light emission from Si is a top issue of current research due to the numerous application fields in optoelectronics, photonics, and sensor technology. Although Si-based light emitters are very attractive and despite the intense research in the last two decades, a sufficiently efficient, electrically driven Si-based light emitter is not yet available. Among the different approaches, rare-earth implanted SiO_2 layers are very promising candidates.[1–3] So we were able to demonstrate strong electroluminescence (EL) from metal-oxide-semiconductor based light emitting diodes (MOSLEDs) doped with Er^{3+},[4] Eu^{3+},[5] Tb^{3+},[6] Ce^{3+},[7] and Gd^{3+} ions.[8] Although in the case of Tb an external quantum efficiency of up to 15% was reached[6] and the lifetime of the devices was improved by more than three orders of magnitude,[9] the MOSLEDs still have deficiencies in terms of efficiency and lifetime if compared with III-IV light emitters or organic LEDs. To overcome these deficiencies the insight into the dynamic processes on a microstructural scale within the light emitter during fabrication and operation is essential. Eu-implanted SiO_2 layers have a lower efficiency than those implanted with Tb, but the existence of two oxidation states, which can be traced indirectly by EL measurements, is a good probe for ongoing processes within the oxide layer.

In this work we investigate the complex dependence of the EL spectrum of Eu-implanted SiO_2 layers on the implantation and annealing conditions. It is shown that the red EL assigned to Eu^{3+} ions is favored by low Eu concentrations, low annealing temperatures, and short annealing times. Based on a more quantitative analysis of the spectra the underlying microstructural processes within the oxide layer will be discussed.

The Eu-implanted MOS structures were fabricated by local oxidation of silicon with 100 nm thick thermally grown SiO_2 on {100} oriented *n*-type silicon wafers. The 100 keV implantation resulted in an Eu profile with a maximum Eu concentration between 0.05% and 6% in the middle of the oxide layer. The samples were subjected to flash lamp annealing (FLA) for 20 ms, rapid thermal annealing (RTA) for 6 s or furnace annealing (FA) for 30 min in nitrogen at temperatures between 900 and 1100 °C. The structure is finally supplied with a SiON protection layer, a transparent front contact made of indium-tin oxide, and a rear contact made of aluminum. For EL measurements a constant injection current of 5 μA at voltages between 140 and 160 V was applied to circular dots with a diameter of 300 μm. The EL spectrum was recorded at room temperature (RT) with a monochromator (Jobin Yvon Triax 320) and a photomultiplier (Hamamatsu H7732-10). The EL decay time was measured by a multichannel scaler (Stanford Research System SR430) under constant voltage pulses. Furthermore, the microstructure of the Eu-implanted SiO_2 layers was analyzed by means of transmission electron microscopy (TEM) with a FEI-Titan instrument.

Figure 1 exhibits the EL spectrum of Eu-implanted MOS devices annealed with RTA at 1000 °C for various Eu concentrations. The spectra consist of a broad EL band in the blue green and at least three EL lines in the red spectral region, which are assigned to Eu^{2+} and Eu^{3+} ions, respectively. The emission of the Eu^{3+} ions is caused by $4f$-intrashell transitions from the $^5D_0$ level to some ^7F_J sublevels, which are indicated in Fig. 1, according to Ref. 10. Since the $4f$ shell is well screened from the chemical environment, these transitions are relatively sharp. However, as the chemical environment strongly varies in the amorphous SiO_2 network, the lines are broader than those usually reported for crystalline matrices.[10] In contrast to this the transition in the Eu^{2+} ion involves an electron that transits from the electronic $5d$ level to the $4f$ shell. As the $5d$ level is much less screened from the chemical environment, the corresponding EL emission is broad, reflecting the variation in the local chemical environment of the Eu^{2+} ion. Furthermore,

[a]Author to whom correspondence should be addressed. Electronic mail: l.rebohle@fzd.de.
[b]Also at Lashkaryov Institute of Semiconductor Physics, National Academy of Sciences of Ukraine, Prospect Nauky 45, 03028 Kiev, Ukraine.

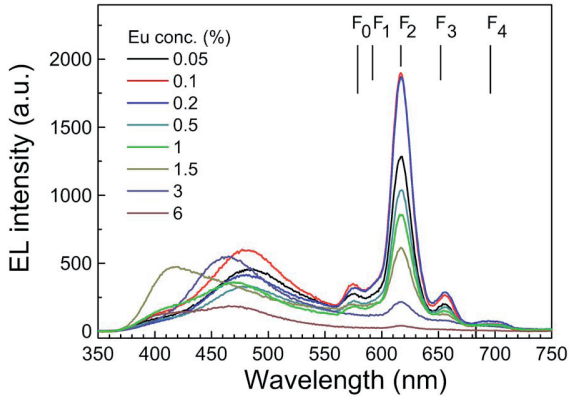

FIG. 1. (Color online) EL spectrum of Eu-implanted MOS devices annealed with RTA at 1000 °C for various Eu concentrations and under an injection current of 5 μA. The black solid lines indicate the position of the $^5D_0$-^7F_J lines ($0 \leqslant J \leqslant 4$) according to Ref. 10.

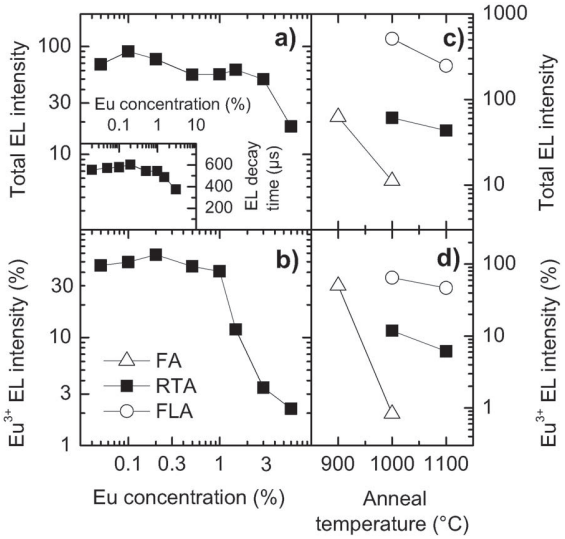

FIG. 2. The dependence of the total EL intensity [(a) and (c)] and the relative intensity of the Eu^{3+} emission in percent [(b) and (d)] of MOS structures on Eu concentrations [(a) and (b)] for RTA at 1000 °C and on annealing [(c) and (d)] for an Eu concentration of 1.5%. The inset shows the EL decay time of the $^5D_0$-$^7F_2$ line for RTA at 1000 °C.

$4f$-intrashell transitions are dipole forbidden resulting in a long decay time for the radiative relaxation, which is not the case for the blue $5d$-$4f$ transition. Consequently, an EL decay time between 350 and 700 μs for the $^5D_0$-$^7F_2$ line and a decay time shorter than 17 μs for the blue EL band is measured. In the latter case the measured decay time was limited by the edge steepness of the voltage pulses we applied to the devices during EL decay time measurements. As can be seen in Fig. 1, the ratio between the blue and red EL emission as well as the detailed structure of the blue-green EL strongly depend on the Eu concentration. For a deeper insight a peak fit analysis of the EL spectra was performed where the EL of the Eu^{3+} ions is modeled by five Gaussian peaks in correspondence to the possible transitions $^5D_0$-^7F_J with $0 \leqslant J \leqslant 4$. An additional Gaussian peak is used in order to consider the asymmetry of the $^5D_0$-$^7F_2$ line. The sum of these peak areas is assumed to represent the EL intensity of the Eu^{3+} ions, and is called the red EL in the following. All other Gaussian peaks are considered to be caused by either Eu^{2+} ions or Si-related defects. It should be noted that the peak positions of the Eu^{3+} peaks are always close to the positions reported in Ref. 10 and that the $^5D_0$-$^7F_2$ line always contains more than 70% of the red EL.

Figure 2 shows the total EL intensity [(a) and (c)] and the relative intensity of the Eu^{3+} emission in percent [(b) and (d)] for MOS structures for different Eu concentrations [(a) and (b)] and different thermal treatments [(c) and (d)]. There the relative intensity of the Eu^{3+} emission is defined as the percentage of the red on the total EL intensity. Whereas there is a smooth decrease in the total EL intensity with Eu concentration (a), the relative intensity of the red EL varies between 0.4 and 0.6 for small concentrations and shows a strong decrease for concentrations higher than 1% (b). The inset of Fig. 2(a) displays the EL decay time of the $^5D_0$-$^7F_2$ line. Furthermore, within one type of annealing both the total EL and the relative intensity of the Eu^{3+} emission decrease with increasing annealing temperature [(c) and (d)]. For a fixed annealing temperature a similar tendency can be observed: a decrease in the total EL and the relative Eu^{3+} intensity with increasing annealing time.

To understand the quenching of the red EL it is necessary to have a closer look to the microstructure of the SiO_2 layer as there are at least three different processes involved. First, during implantation Si and oxygen are released from the SiO_2 network either by nuclear collisions or by electronic energy deposition leading to bond breaking. In the following phase of annealing the released oxygen can be either reintegrated in the SiO_2 network or can be used to oxidize Eu. The formation enthalpy at RT for EuO, Eu_2O_3, and SiO_2 is in the order of -565 kJ mol^{-1},[11] -1650 kJ mol^{-1} (that is -825 kJ mol^{-1} per Eu atom)[12] and -910 kJ mol^{-1},[13] respectively. Although SiO_2 has the lowest value, it has also the highest demand on oxygen per reactant (Si or Eu). Indeed, there will be a competition for oxygen leading also to a local excess of Si that in turn triggers the formation of oxygen deficiency centers (ODCs). The ODCs are known to be efficient luminescence centers in the blue,[14,15] which can give a contribution to the total EL intensity. This process becomes more intense with increasing implantation dose, and as a consequence the relative Eu^{3+} intensity decreases with increasing Eu concentration. However, Tb-implanted and Gd-implanted SiO_2 layers that were prepared with similar parameters show either no or only a weak EL in the blue green,[6,8] which leads to the conclusion that the complex dynamics in the blue-green spectral region is mainly due to Eu.

The second quenching process is the preference of EuO compared to Eu_2O_3. Although the formation enthalpy of Eu_2O_3 (Eu^{3+} configuration) is higher than that of EuO (Eu^{2+} configuration), the supply of oxygen that is available for the oxidation of Eu determines whether EuO or Eu_2O_3 dominates. At low Eu concentrations a single Eu atom will find enough oxygen in its local environment to achieve a Eu_2O_3 configuration. With increasing Eu concentration the average distance between neighboring Eu ions decreases, and a competition of the Eu ions for oxygen starts which finally will shift the weight from Eu^{3+} to Eu^{2+} for high Eu concentrations. For RTA at 1000 °C the EL decay time of the $^5D_0$-$^7F_2$ line drops down continuously from 606 μs for 0.2% Eu to 375 μs for 3% Eu. The intensity of the red EL decreases in a similar way, but is stronger than implied by the ratio of the corresponding EL decay times. Thus the EL quenching caused by additional nonradiative relaxation processes of ex-

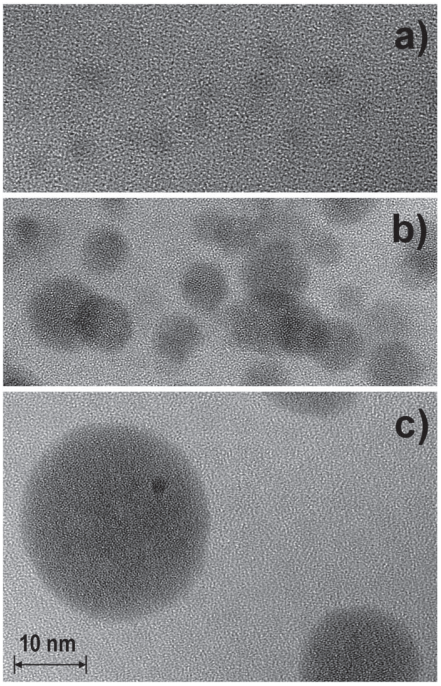

FIG. 3. Bright field cross section TEM images showing Eu/Eu oxide clusters in the SiO_2 layer for 1.5% Eu and annealed at 1000 °C by FLA (a), RTA (b), and FA (c). All images have the same magnification.

cited Eu^{3+} ions will give a minor contribution to the total quenching only.

The third development to be considered is the formation and the subsequent ripening of Eu/Eu oxide clusters. In Fig. 3 the development of these clusters is shown for an annealing temperature of 1000 °C. After FLA 20 ms only small amorphous Eu/Eu oxide clusters with diameters between 2 and 3 nm are observed. Whereas the amorphous clusters enlarge to diameters between 7 and 9 nm for RTA 6 s, huge and partly crystallized clusters with sizes around 25 nm can be found for FA 30 min. An analogous behavior is observed for the temperature dependence (not shown), so that a clear increase in the cluster size with increasing annealing temperature and time can be asserted. Because of the higher dielectric constant of Eu oxide[16] compared with SiO_2 and the continuity of the dielectric displacement, the electric field within an Eu oxide cluster is lower than in the SiO_2 matrix. Lower electric fields are not high enough to accelerate electrons to energies needed for the excitation of Eu ions, for which reason Eu ions inside a cluster are assumed to be optically inactive. Hot electrons moving in the conduction band of SiO_2 are able to excite Eu ions that are located at the surface of an Eu/Eu oxide cluster only. With increasing cluster size the fraction of Eu ions located at the cluster surface will decrease, and in turn a decrease in the total EL intensity with increasing annealing temperature time, namely, in the order FLA, RTA, and FA, is expected. Indeed, such a behavior is observed in Fig. 2(c). Moreover, because of the high Eu concentration within and on the surface of the clusters Eu will predominantly occur in the divalent stage. So if more and more Eu atoms are bound in clusters the weight will shift more and more to the blue EL. Finally, a certain fraction of Eu will diffuse toward the interfaces of the SiO_2 layer under long-time annealing (not shown) and cannot be excited electrically anymore. It has to be noted that the question, whether the clusters consists of Eu, Eu_2O_3 or EuO_x with $0<x<1.5$, is still under investigation. However, on the basis of the thermodynamic properties of Eu and its oxide we assess that the formation of Eu oxide clusters are more probable than that of Eu clusters.

In summary we have demonstrated that Eu-implanted SiO_2 layers exhibit a strong EL that is both due to the emission from Eu^{2+} and Eu^{3+} states. The red EL due to Eu^{3+} ions is favored by low Eu concentrations, lower annealing temperatures, and shorter annealing times. The increase in the blue portion of the EL with larger Eu concentrations, annealing temperatures, and annealing times is accompanied by a reduction in the total EL intensity. Although not all details are known, this behavior can be well explained by a shorter supply of oxygen for higher Eu concentrations and the growth of Eu/Eu oxide clusters with increasing anneal temperatures and times.

The authors would like to thank A. Dahmen of the Forschungszentrum Jülich and the Rossendorf Implantation Group for ion implantation and H. Felsmann, C. Neisser, and G. Schnabel for their careful semiconductor preparation work.

[1] C. Buchal, S. Wang, F. Lu, R. Carius, and S. Coffa, Nucl. Instrum. Methods Phys. Res. B **190**, 40 (2002).
[2] A. Irrera, M. Miritello, D. Pacifici, G. Franz, F. Priolo, F. Iacona, D. Sanfilippo, G. Di Stefano, and P. G. Fallica, Nucl. Instrum. Methods Phys. Res. B **216**, 222 (2004).
[3] F. Priolo, C. D. Presti, G. Franzò, A. Irrera, I. Crupi, F. Iacona, G. Di Stefano, A. Piana, D. Sanfilippo, and P. G. Fallica, Phys. Rev. B **73**, 113302 (2006).
[4] J. M. Sun, W. Skorupa, T. Dekorsy, M. Helm, and A. M. Nazarov, Opt. Mater. (Amsterdam, Neth.) **27**, 1050 (2005).
[5] S. Prucnal, J. M. Sun, W. Skorupa, and M. Helm, Appl. Phys. Lett. **90**, 181121 (2007).
[6] J. M. Sun, W. Skorupa, T. Dekorsy, M. Helm, L. Rebohle, and T. Gebel, J. Appl. Phys. **97**, 123513 (2005).
[7] J. M. Sun, S. Prucnal, W. Skorupa, M. Helm, L. Rebohle, and T. Gebel, Appl. Phys. Lett. **89**, 091908 (2006).
[8] J. M. Sun, S. Prucnal, W. Skorupa, T. Dekorsy, A. Mücklich, M. Helm, L. Rebohle, and T. Gebel, J. Appl. Phys. **99**, 103102 (2006).
[9] J. M. Sun, L. Rebohle, S. Prucnal, M. Helm, and W. Skorupa, Appl. Phys. Lett. **92**, 071103 (2008).
[10] G. H. Dieke, *Spectra and Energy Levels of Rare Earth Ions in Crystals* (Interscience, New York, 1968).
[11] E. J. Huber and C. E. Holley, J. Chem. Thermodyn. **1**, 301 (1969).
[12] G. C. Fitzgibbon, E. J. Huber, and C. E. Holley, J. Chem. Thermodyn. **4**, 349 (1972).
[13] M. Nagamori, J.-A. Boivin, and A. Claveau, J. Neurosci. Res. **189**, 270 (1995).
[14] L. Rebohle, J. von Borany, H. Fröb, and W. Skorupa, Appl. Phys. B: Lasers Opt. **70**, 1 (2000).
[15] A. N. Trukhin, M. Goldberg, J. Jansons, H.-J. Fitting, and I. A. Tale, J. Non-Cryst. Solids **223**, 114 (1998).
[16] H. Nakane, A. Noya, S. Kuriki, and G. Matsumoto, Thin Solid Films **59**, 291 (1979).